ACS APPLIED MATERIALS & INTERFACES

Research Article

www.acsami.org

Enhanced Biocompatibility of PLGA Nanofibers with Gelatin/Nano-Hydroxyapatite Bone Biomimetics Incorporation

Daowei Li,[∥,†] Haizhu Sun,[∥,‡] Liming Jiang,[†] Kai Zhang,[§] Wendong Liu,[§] Yang Zhu,[†] Jiaozi Fangteng,[†] Ce Shi,[†] Liang Zhao,[†] Hongchen Sun,[†,*] and Bai Yang[§]

[†]Department of Pathology, School of Stomatology, Jilin University, Changchun 130021, China

[‡]Faculty of Chemistry, Northeast Normal University, Changchun 130024, China

[§]State Key Laboratory of Supramolecular Structure and Materials, Jilin University, Changchun 130012, China

ABSTRACT: The biocompatibility of biomaterials is essentially for its application. The aim of current study was to evaluate the biocompatibility of poly(lactic-*co*-glycolic acid) (PLGA)/gelatin/nanohydroxyapatite (n-HA) (PGH) nanofibers systemically to provide further rationales for the application of the composite electrospun fibers as a favorable platform for bone tissue engineering. The PGH composite scaffold with diameter ranging from nano- to micrometers was fabricated by using electrospinning technique. Subsequently, we utilized confocal laser scanning microscopy (CLSM) and MTT assay to evaluate its cyto-compatibility in vitro. Besides, real-time quantitative polymerase chain reaction (qPCR) analysis and alizarin red staining (ARS) were performed to assess the osteoinductive activity. To further test in vivo, we implanted either PLGA or PGH composite scaffold in a rat subcutaneous model. The results demonstrated that PGH scaffold could better support osteoblasts adhesion, spreading, and proliferation and show better cyto-compatibility than pure PLGA scaffold. Besides, qPCR analysis and ARS showed that PGH composite scaffold exhibited higher osteoinductive activity owing to higher phenotypic expression of typical osteogenic genes and calcium deposition. The histology evaluation indicated that the incorporation of Gelatin/nanohydroxyapatite (GH) biomimetics could significantly reduce local inflammation. Our data indicated that PGH composite electrospun nanofibers possessed excellent cyto-compatibility, good osteogenic activity, as well as good performance of host tissue response, which could be versatile biocompatible scaffolds for bone tissue engineering.

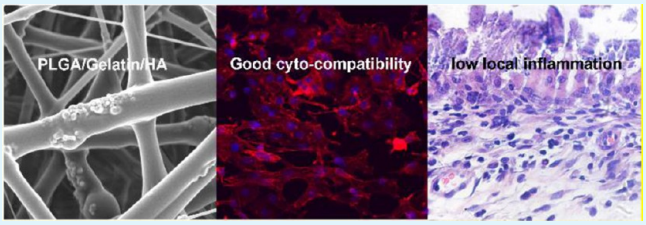

KEYWORDS: *electrospun nanofibers, poly(lactic-co-glycolic acid), gelatin/nanohydroxyapatite, bone biomimetics, bone tissue engineering, biocompatibility*

1. INTRODUCTION

It is important to develop biocompatible substitutes by tissue engineering in order to repair, maintain, and improve tissue function. The biocompatibility of a tissue engineered scaffold refers to three interrelated aspects: (1) the scaffold performed its desired function and generated best cellular or tissue response in regard to a medical therapy, (2) without eliciting any undesirable effects in that therapy, and (3) obtaining good clinically outcome of that therapy.[1] Thus, it requires the scaffold to be not only safe but also well-functioning. Therefore, the biocompatibility of a scaffold is crucial for its application.

Recently, electrospun nanofibrous scaffolds have gained tremendous attention because their micro- to nanoscale features are similar to the fibrous architecture of the ECM and been designed to serve as ideal bone substitutes.[2−4] In addition, the high surface area-to-volume ratio and high porosity of electrospun nanofibers make it possible to serve as delivery vehicles for drugs, genes, growth factors, and other bioactive molecules.[4−6] Various biodegradable synthetic and natural polymers or compositions have been electrospun to fabricate nanofibrous scaffolds that are utilized as cell-supporting matrices for bone regeneration.[7−10] Poly(lactic-*co*-glycolic acid) (PLGA)-based electrospun nanofibrous scaffolds have been investigated by a number of research groups as well as our group for tissue engineering.[11−14] However, the poorly bioactivity and serious local inflammation induced by the acidic degradation products of PLGA nanofibers, which limited its applications.[11,15] Composite electrospun nanofibers containing nanohydroxyapatite have been shown to stimulate higher specific osteogenic genes expression of osteoblastic/stem cells.[13,16,17] Moreover, studies have demonstrated that electrospun nanofibers made of hydroxyapatite/gelatin exhibited significantly enhanced osteoblasts responses.[18] Besides, given that bone is an organ in which collagen fibril forms a scaffold for arrangement of hydroxyapatite (HA) crystals orderly,[19] the gelatin/nanohydroxyapatite(n-HA)(GH) nanocomposite could mimic the natural bone matrix to some extent.[18,20] Therefore, we expect to improve the biocompatibility of PLGA electro-

Received: March 25, 2014
Accepted: May 30, 2014
Published: May 30, 2014

   dx.doi.org/10.1021/am5017792 | *ACS Appl. Mater. Interfaces* 2014, 6, 9402−9410

spun nanofibrous by introduction of GH biomimetics. Although researchers had reported that the blending GH to PLGA can modulate the inherent hydrophilicity property, degradation behaviors, and tensile strength that were more suitable for bone cell growth.[12] However, a systemic study regarding to biocompatibility issues of GH bone mimetics modified PLGA nanofibers should be performed before applying in clinical trials.

In the present study, we investigated the adhesion, proliferation, and osteogenic differentiation of osteogenitor cells on the scaffold to assess the cytocompatibility and osteogenic activity of the scaffold in vitro. Moreover, we also determined the host tissue responses of the scaffold in vivo. Our research indicated that electrospun PGH scaffold possessed excellent cyto-compatibility, good osteogenic activity, as well as good performance of host tissue response, which could be a versatile scaffold for bone tissue engineering.

2. MATERIALS AND METHODS

2.1. Scaffolds Preparation. PLGA and PGH nanofibrous scaffolds were fabricated via electrospinning. Gelatin/n-HA (GH) bone biomimetics was prepared by mixing gelatin solution with n-HA under vigorously stirring for more than 48 h. PLGA electrospun solution was prepared by dissolving PLGA (ratio of lactic to glycolic acid = 85:15, molecule weight 106 000 Da; Changchun Institute of Applied Chemistry, Chinese Academy of Sciences, China) in 1,1,1,3,3,3-hexafluoro-2-propanol (HFIP, Sigma-Aldrich, U.S.A.) with a 10% (w/v) concentration. For fabricating PGH fibers, the electrospun solution was prepared as follows: 0.06 g nanohydroxyapatite (HA, diameter less than 200 nm, Sigma-Aldrich, U.S.A.) was uniformly dispersed in 3 mL HFIP under magnetic stirring for 24 h. 0.3 g gelatin was then added to get a concentration of 10% (w/v). The mixtures were stirred vigorously for more than 48 h to make n-HA closely integrated with gelatin due to the interaction between the calcium ions of n-HA and the carboxylic group of gelatin.[20] Besides, 0.7 g PLGA was dissolved in 7 mL HFIP with a 10% (w/v) concentration. Finally, the two solutions were mixed together under stirring for 6 h to get the electrospun solution. A high voltage of 15 kV was applied to the solutions. A mandrel covered with aluminum foil was used to collect the spouted nanofibers, which were located at a 15 cm distance from the positive electrode. The flow rate was set to 0.5 mL h^{-1}. The electrospun nanofibers were dried in air at room temperature for several days.

2.2. SEM and AFM Image. Scanning electron microscopy (SEM; JEOL FESEM 6700F, Tokyo, Japan) was performed to examine the surface morphology of nanofibrous scaffolds. The specimens were sputtered with a thin layer of Pt to reduce the surface charging of the samples. The SEM was operated at 3 kV to observe the surface features of the nanofibers. Image-Pro Plus (Media Cybernetics, Rockville, MD, U.S.A.) was used to quantitatively measure fiber diameter and distribution. Besides, the surface roughness of nanofibers was evaluated by Atomic force microscope (AFM) image at tapping mode.

2.3. Wettability and Swelling Ratio of the Scaffolds. The wettability of PLGA and PGH fibers were characterized by measuring the static water contact angles at room temperature. Besides, the swelling ratio of the scaffolds was measured by water uptake capacity. The scaffolds with known weights (denoted as M1) were put in weighing bottle containing 5 mL medium (pH 7.4) each and incubated for 24 h at 37 °C. This was aim to simulate the swelling process in vivo environment. Afterward, the specimens were placed on filter paper to remove water on the surfaces and then weighted in wet condition (denoted as M2). The swelling ratio of each sample was calculated by using the following equation.

$$\text{swelling ratio}\ (\%) = (M1 - M2)/M2 \times 100\% \quad (1)$$

2.4. Cell Spreading, Attachment, and Proliferation Assays. The MC3T3-E1 subcolon 14 cell line which was derived from C57BL/6 mouse. They have special behavior that is similar to primary calvarial osteoblasts. The medium for growth of the cell line was α modification of Eagle's Minimum Essential Medium (α-MEM; Life Technologies, Carlsbad, CA, U.S.A.) (without ascorbic acid) containing 10% fetal bovine serum (FBS; Life Technologies, Carlsbad, CA, U.S.A.). The cells were placed under standard cell culture conditions, and the medium was changed every 2−3 days.

PLGA and PGH nanofibrous mats were prepared to match the inside diameter of 6 well cell culture plate. Then the scaffolds were irradiated with UV light for 2 h and placed into the culture plate. Besides, a sterile iron loop that also matchs the inside diameter of 6 well cell culture plate was used to fix the nanofibrous mats. Then, MC3T3-E1 cells were seeded on the surface of the scaffolds at 2×10^4 MC3T3-E1 cells/cm^2 and cultured for 24 h under standard cell culture conditions. For cell spreading and attachment examination, cytoskeletal of cells cultured on the nanofibrous mats was stained with rhodamine phalloidin (Invitrogen, Eugene, OR, U.S.A.) and nuclei was counterstained by 4′,6-diamidino-2-phenylindole (DAPI; Sigma-Aldrich, U.S.A.) at 6 and 24 h time points, followed by an examination of attached cell number under confocal laser scanning microscopy (CLSM) (FluoViewTM FV1000, Olympus, Japan). To ensure a representative count, five locations at up, down, left, right, and middle per sample were photographed. The number and area of the stained cells were measured and quantitated using Image-Pro plus software (IPP; Media Cybernetics, Rockville, MD, U.S.A.).

Cell proliferation on the nanofibrous scaffolds was investigated by using the 3-[4,5-dimethylthiazol-2-yl]-2,5-diphenyl tetrazolium bromide (MTT; AMRESCO, U.S.A.) assay. MC3T3-E1 cells were seeded on the scaffolds and cultured at a density of 1×10^4 cells/cm^2 in 96 well culture plates. At prefixed culture time points, 20 μL of MTT solution (5 mg/mL in PBS) was added to each well, followed by incubation at 37 °C cell incubator for 4 h. The supernatant was then removed, and the formed formazan crystals were dissolved by dimethyl sulfoxide. After the incubation period, the samples were pipetted out into another 96 well plates. The absorbance was determined at 570 nm using a microplate reader (RT-6000, Lei Du Life Science and Technology Co, Shenzhen, China).

2.5. Differentiation of BMSCs. Rat bone marrow stromal stem cells (BMSCs) were isolated from the femurs of young (4 weeks old) Wistar rat. Total bone marrow cells were pumped out using a 20 mL syringe and plated in cell culture dish (NEST, China). The medium for growth of BMSCs was α-MEM containing 10% FBS, 100 U/mL penicillin (Life Technologies, Carlsbad, CA, U.S.A.), and 100 mg/mL streptomycin (Life Technologies, Carlsbad, CA, U.S.A.). The cells were cultured under standard cell culture conditions, and the medium was changed 3 days later. Passage third isolated BMSCs were seeded at a density of 1.5×10^5 cells/sample on scaffolds in 6 well cell culture plates. The growth media was replaced with osteogenic conditioned medium of α-MEM containing 10% FBS, 10^{-8} M dexamethasone, 10 mM sodium β-glycerol phosphate and L-ascorbic acid (50 mg/mL), and the medium was changed every 3 days. On days 7, 14, and 21 after cell seeding, samples were taken out from the 6 well plates and the total RNA of the cells on the scaffolds was extracted by Trizol reagent (Invitrogen, U.S.A.). Specific osteogenic gene expression of type I collagen (Col1), alkaline phosphatase (ALP), and Runt-related transcription factor 2 (Runx2) was analyzed by Real-time Quantitative Polymerase Chain Reaction (qPCR), and β-actin was employed as the house keeping gene. The experiments were performed in triplicate. The primer sequences used for this analysis were as follows: Runx2, 5′-CATGGCCGGGAATGATGAG-3′/5′-TGTGAAGACCGTTATGGTCAAAGTG −3′; Alp, 5′- CATCGCCTATCAGCTAATGCACA-3′/5′-ATGAGGTCCAGGCCATCCAG-3′; Col1, 5′-GACATGTTCAGCTTTGTGGACCTC-3′/5′-AGGGACCCTTAGGCCATTGTGTA-3′; β-actin, 5′-GGAGATTACTGCCCTGGCTCCTA-3′/5′-GACTCATCGTACTCCTGCTTGCTG-3′. Primers were synthesized commercially (Takara Bio, Dalian, China).

Alizarin red staining (ARS) was performed to evaluate the amount of ECM produced by BMSCs qualitatively and quantitatively. On day 21, the scaffolds seeded with BMSCs were fixed in 90% ice-cold ethanol for 10 min. Then, the samples were washed thrice with distilled water and stained with ARS (0.1%) for 30 min at 37 °C. After washing several times with distilled water, the scaffolds were examined under upright optical microscope (Olympus BX51, Japan). The ARS was then dissolved by 10% cetylpyridinium chloride monohydrate (Sigma-Aldrich, U.S.A.) (dissolved in distilled water) and quantified using a microplate reader (RT-6000, Lei Du Life Science and Technology Co, Shenzhen, China) at 540 nm wavelength. Deionized water and PLGA/Gelatin/HA without cell culture group were analyzed as the control to rule out the effects of HA on calcium outcomes.

2.6. The Biocompatibility of the Scaffolds in Vivo. Twenty-four six-month-old male Wistar rats were used to create dorsal incision models, and the procedures were approved by Jilin University Animal Care and Use Committee. The rats were randomly divided into two groups: a PLGA group and a PGH group (n = 12). The experimental procedures were as follows: rats were anesthetized with isoflurane and Lidocaine. The surgical sites were cleaned and disinfected with 70% ethanol and iodine scrub. Two paravertebral incisions (1.5 cm each) per rat were made approximately 1 cm lateral to the vertebral column to expose the dorsal subcutis. Subcutaneous pockets were created by blunt dissection. Both the pockets were used for implantation of the same scaffold. After insertion of an implant, the incisions were then sutured with 3−0 sutures. After the surgery, all rats were raised in the same environment as before and received an analgesic and an antibiotic for 3 days.

Animals were allowed to survive for 14 days; then, the rats were anesthetized and euthanized. The tissue-covered specimens were collected and fixed in 4% paraformaldehyde, dehydrated in a graded series of ethanol. The specimens were incised along the major axis and embedded in paraffin. Slices (5 μm) of maximum cross-section of each sample were prepared for hematoxylin and eosin (H&E) and immunochemistry staining. Herein, infiltrated macrophages and monocytes were identified by CD68 antibody immunochemistry staining. Histological evaluation was performed by two independent examiners according to a histological grading scale as shown in Table 1.[21,22] Four representative areas on major and minor axis of fibrous capsules in each section were determined to quantitatively assess the fibrous capsule quality.

Table 1. Histological Grading Scale for Inflammatory Immune Response

(1) capsule quality	score
fibrous, not dense, resembling connective or fat tissue	4
fibrous, but immature, showing fibroblasts and little collagen	3
granulous and dense, containing both fibroblasts and many inflammatory cells	2
mass inflammatory cells with little or no signs of connective tissue organization	1
cannot be evaluated because of infection or other factors	0
(2) capsule thickness	score
1−4 fibroblasts	4
5−9 fibroblasts	3
10−30 fibroblasts	2
>30 fibroblasts	1
not applicable	0
(3) cell infiltration	score
only fibroblasts contact the surface	4
scattered macrophages and leucocytes are present	3
one layer of macrophages and leucocytes are present	2
multiple layers of macrophages and leucocytes present	1
cannot be evaluated	0

2.7. Statistical Analysis. Quantitative values were averaged and expressed as mean-standard deviation. Statistical differences were performed by one-way analysis of variance (ANOVA). Differences were considered statistically significant at $p < 0.05$. Each experiment was repeated 3 times or more.

3. RESULTS

3.1. Characterization of Nanofibrous Scaffolds. SEM images showed that both PLGA and PGH composite nanofibers presented randomly oriented morphology (Figure 1A, B). The n-HA particles were well distributed on the surface

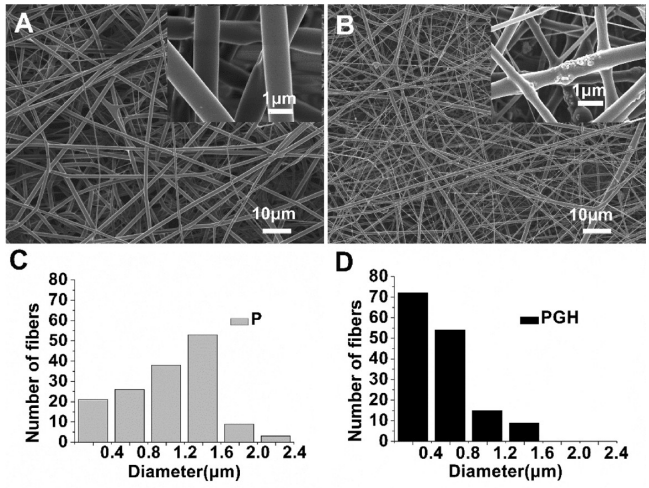

Figure 1. SEM images of PLGA (A) and PLGA/Gelatin/n-HA (B) nanofibers. Fiber diameter distribution of PLGA (C) and PLGA/Gelatin/n-HA (D) nanofibers. P: PLGA. PGH: PLGA/Gelatin/n-HA.

of the PGH composites while pure PLGA fibers were smooth. The distributions of fiber diameter for both scaffolds are showed in Figure 1C, D. Fiber diameter decreased with the addition of GH, which implied that the PGH scaffold might possess larger surface area. The porous structure of the scaffolds would be favorable for nutrients and metabolic waste exchange.

We used AFM to evaluate nanoscale surface topographies of nanofibers. The calculated root mean squared (RMS) roughness of the PLGA nanofibers surface was 3.4 nm. This value increased to 10.1 nm after GH biomimetics incorporation (Figure 2A, B). This was confirmed by SEM image (Figure 1A, B). This result could be explained by the distributed n-HA on the surfaces of nanofibers.

The wettability of the scaffolds was examined by static water contact angles analysis. The contact angle had no differences when liquid drop attached on the scaffolds at the beginning, as shown in Figure 3A. However, the water infiltrated quickly 12 s later on the PGH composites scaffold, while no change on the PLGA scaffold. The results implied that the PGH surface were more hydrophilic. Besides, the water uptake ratio of blended nanofibrous scaffold was extremely higher. The swelling ratio of PGH composite scaffold was 386.12 ± 20.77%, while the pure PLGA nanofibers group was only 46.87 ± 10.66% (Figure 3B).

3.2. Cell Spreading, Attachment, and Proliferation on the Scaffolds. Figure 4 showed the cell behavior on the scaffolds at 6 and 24 h time point of culture. Fluorescent phalloidin was used to mark the actin filaments of cells grown on the scaffolds and the nucleus was counter-stained with DAPI. It was found that the adhered MC3T3-E1 cells stretched better on the PGH composite group than on the pure PLGA

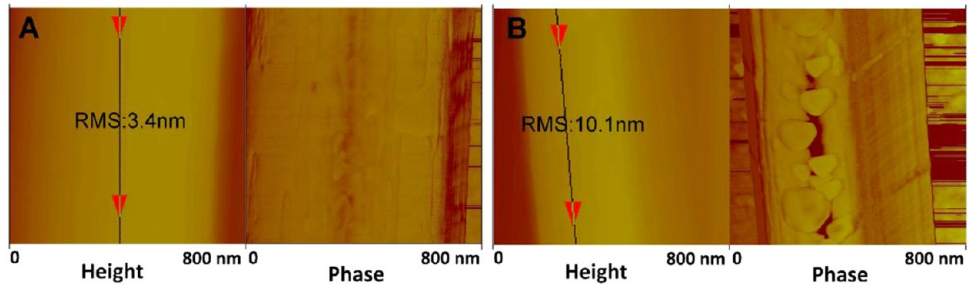

Figure 2. Height and the corresponding phase images from tapping mode AFM of electrospun pure PLGA (A) and PLGA/Gelatin/n-HA (B) nanofibers. RMS: root mean squared.

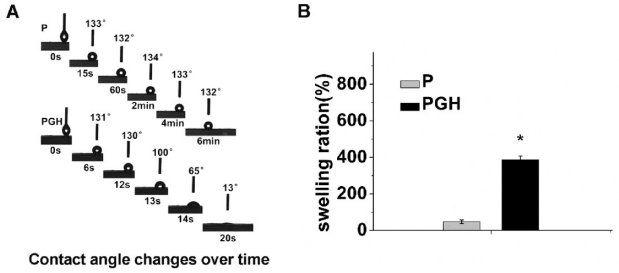

Figure 3. Static contact angle changes over time (A) and swelling ratio of the two scaffolds (B), P: PLGA scaffold. PGH: PLGA/gelatin-hydroxyapatite scaffold. *Represents statistically significant difference ($P < 0.05$).

group (Figure 4). There were more attached cell numbers on the PGH scaffold than on pure PLGA scaffold (Figure 4E, $p < 0.05$). At 6 h, the cells on the PGH scaffold have spread out and possessed much longer filopodial attachments compared to pure PLGA scaffold (Figure 4A, B, F). Cells on PGH scaffold more tightly packed when compared with PLGA scaffold at the 24 h (Figure 4C, D). These results indicated that the incorporation of GH into PLGA scaffold markedly increased cellular adherence, attachment, and spreading.

The proliferation of MC3T3-E1 cells on the two scaffolds was determined by MTT assays. At 1, 3, and 5 days after seeding, the proliferation of MC3T3-E1 cells on the nanofibrous PGH composites was significantly higher than PLGA scaffold (Figure 5, $p < 0.05$). This indicated that the PGH scaffold was more suitable for osteoblasts growth as compared

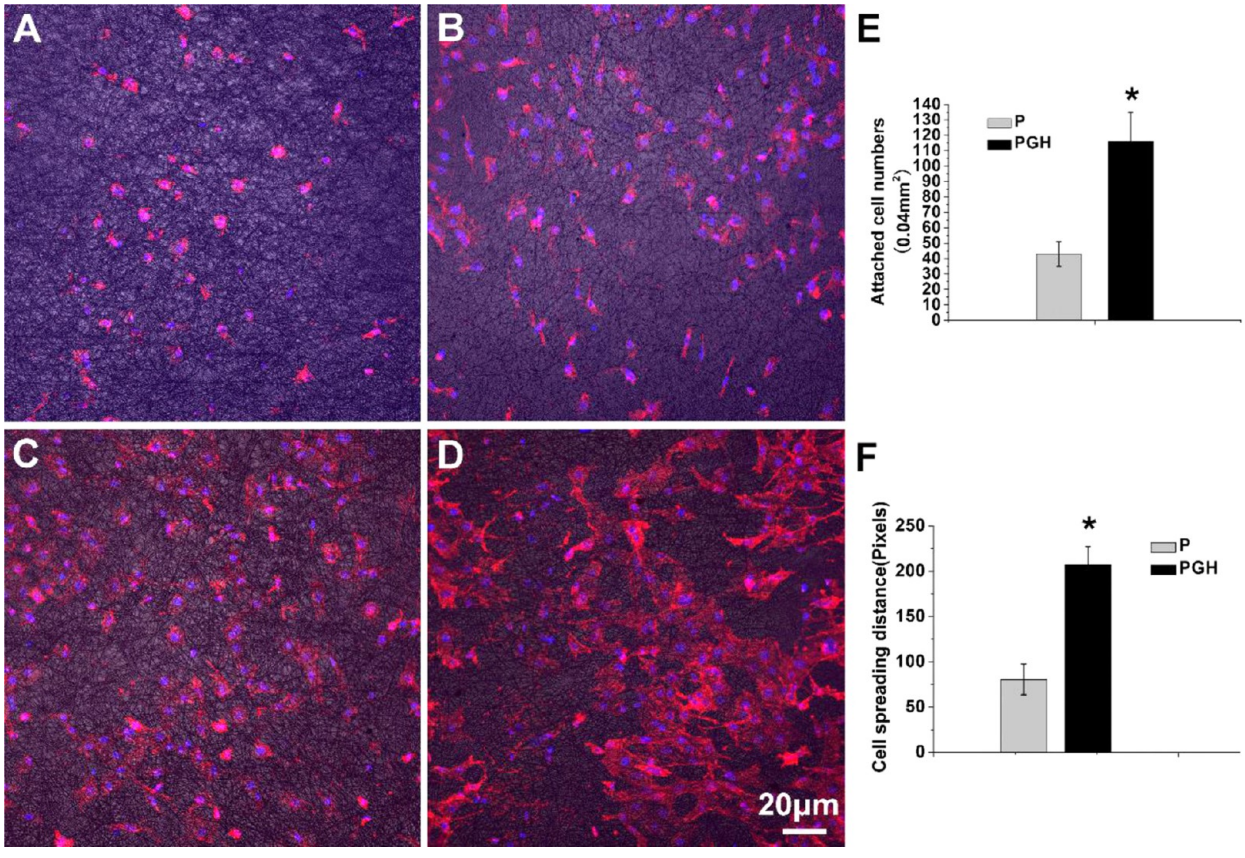

Figure 4. Responses of MC3T3-E1 cells on the scaffolds at 6 h (A, B) and 24 h (C, D) time points under CLSM observation. Quantitative analysis of MC3T3-E1 cells attachment (E) and spreading (F) at 6 h time point. P: PLGA. PGH: PLGA/Gelatin/n-HA. *Represents statistically significant difference ($P < 0.05$).

dx.doi.org/10.1021/am5017792 | ACS Appl. Mater. Interfaces 2014, 6, 9402−9410

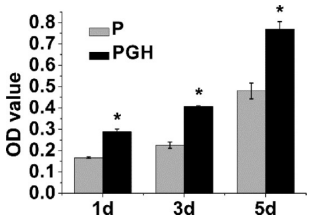

Figure 5. Proliferation of MC3T3-E1 cell on scaffolds during a 5-day culture period. P: PLGA. PGH: PLGA/gelatin/n-HA. *Represents statistically significant difference ($p < 0.05$).

to pure PLGA scaffold. The biocompatibility of the PLGA based electro-nanofibers was improved with adding of GH bone biomimetics.

3.3. Differentiation of BMSCs on the Scaffolds. The effects of the scaffolds on progenitor cells differentiation were determined by qPCR and Alizarin red staining assays. When BMSCs were cultured in osteogenic medium containing ascorbic, β-glycerophosphate and dexamethasone for up to 21 days, we evaluated the expression of specific osteoblastic genes by qPCR (Runx2, Col1, and Alp). As seen in Figure 6, an up-regulated expression level of osteogenic genes was observed on PGH group as compared to the pure PLGA group. These data indicated that the presence of GH bone biomimetics has accelerated osteogenic differentiation of BMSCs.

The mineral deposition on the scaffolds was investigated both qualitatively and quantitatively (Figure 7). Alizarin red staining assay showed that there was more calcium deposition on the PGH scaffold compared with PLGA group (Figure 7A, B). The quantitative evaluation of calcium deposition confirmed PGH has enhanced osteogenic activity (Figure 7C). The results demonstrated the positive effects of GH on osteogenic differentiation of BMSCs.

3.4. Biocompatibility of the Scaffolds In Vivo. The inflammatory immune response to pure PLGA and composite PGH scaffolds were evaluated after a 2-week subcutaneous implantation period in Wistar rat in vivo. Representative H&E and CD68 staining sections of the scaffolds are shown in Figure 8. Histological observation showed that there were fibrous capsules surrounding all the scaffolds. Besides, fibroblasts and inflammation cells infiltrated at the interface between fibrous capsules and the scaffolds. The presence of multilayer multinuclear cells were found in PLGA group, whereas there were only scattered multinuclear cells in the PGH composite scaffold group. The CD68 antibody immunochemistry staining indicated that the multinuclear cells were macrophages. Histological grading results indicated that there was a significant reduction of inflammatory cells infiltration between the scaffolds remnants and the fibrous capsule walls with incorporation of GH (Figure 8G) ($p < 0.05$). However, the capsule quality and thickness of PLGA group were similar to PGH composite scaffold. The capsule mainly consisted of multiple layers (6−10 layers) of fibroblasts. The results indicated that PGH nanofibers scaffold showed good biocompatibility in vivo.

4. DISCUSSION

Biocompatible scaffold, living cells and bioactive molecules are key factors of tissue engineering.[23] Bone substitute scaffold should not generate any clinically significant undesirable effects in the host. Furthermore, the scaffold should produce favorable effects in that patient.[1] Herein, we performed a series of experiments to determine the cell guidance features of the composite PGH scaffold in vitro, as well as host tissue response in vivo which provided further rationales for the application of the composite PGH electrospun fibers as a favorable platform for bone tissue engineering.

Randomly oriented nanofibers of PLGA and PGH scaffolds were obtained by the electrospinning technique. Due to the interaction between the calcium ions of HA and the carboxylic group of gelatin, we got a very homogeneous electrospun solution.[20] It is the basis to obtain good electrospun fibers. The morphologies of the obtained nanofibers and their diameter distribution were measured and tabulated as shown in Figure 1. It is noticed that the diameter of the fibers decreased with adding GH. One possible reason is that the viscosity of the composite solution declined after the addition of GH. The other is that the amino acids of the gelatin increased the charge density of the jet, which could enhance the stretching force and the self-repulsion during electrospinning.[24] The height and the corresponding phase images of nanofibers from tapping mode AFM (Figure 2) showed that the adding of GH increased surface roughness of PLGA nanofibers. This may due to the n-HA, which deposited on the surface of nanofibers (Figure 2B). The increased nanoscale roughness combined with arginine-glycine-aspartic acid (RGD) sequences within gelatin may promote osteoblasts adhesion and function.[25]

The static water contact angle assay indicated that the PGH composite scaffold were more hydrophilic (Figure 3A). Moreover, the water uptake was significantly increased with the addition of GH due to the hydrophilicity of gelatin and HA (Figure 3B).[26,27] It may contribute to the nutrition exchange in the scaffolds. The hydrophilic characteristic of the scaffolds is also better for cell adhesion.[28]

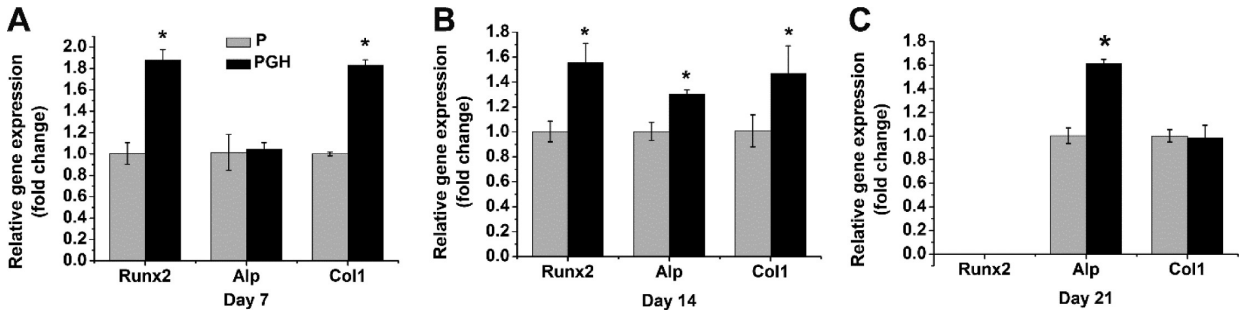

Figure 6. Quantitative analysis of Runx2, Col1, and ALP expression on days 7 (A), 14 (B), and 21 (C) expression in BMSCs cultured on scaffolds by Q-PCR. *Represents statistically significant difference ($P < 0.05$), P: PLGA. PGH: PLGA/gelatin/n-HA.

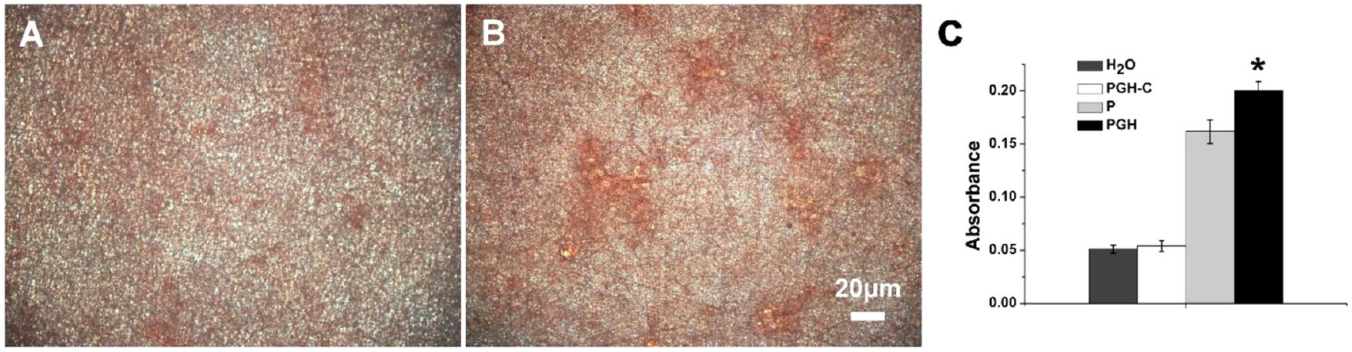

Figure 7. Mineral deposition of bone marrow mesenchymal stem cells on day 21 and quantification. (A) PLGA group, (B) PLGA/gelatin/n-HA group, (C) Quantification of deposited calcium. H_2O: deionized water group. PGH-C: group of PLGA/gelatin/HA without cell culture. P: PLGA group with cell culture. PGH: PLGA/gelatin/n-HA group with cell culture. *Represents statistically significant difference ($p < 0.05$).

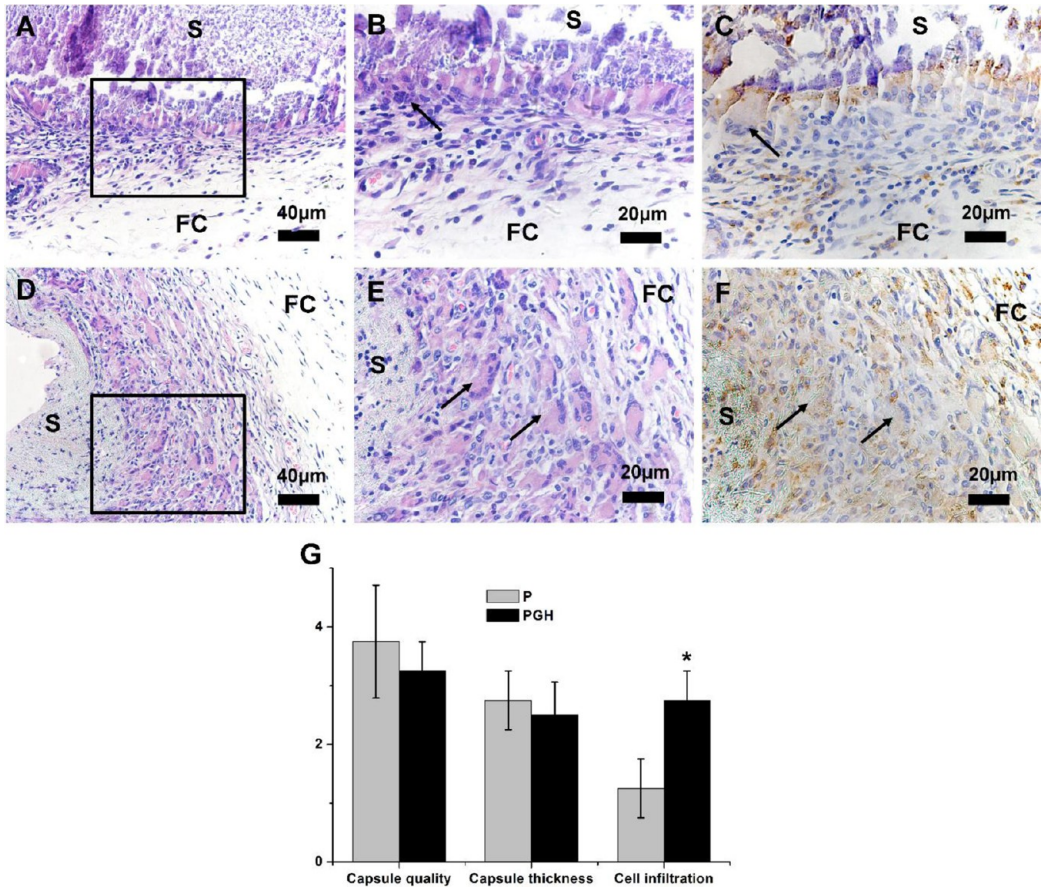

Figure 8. Histological response and grading of two scaffolds after 2-week subcutaneous implantation. (A, B, C) PLGA group, (D, E, F) PLGA/gelatin/n-HA group, (G) histological grading of host tissue response; (A, B, D, E) HE staining, (C, F) CD68 immunohistochemistry staining of macrophage and monocyte. FC: Fibrous capsule wall. S: scaffold remnants. Black arrow: infiltrated macrophage. P: PLGA. PGH: PLGA/gelatin/n-HA. *Represents statistically significant difference ($p < 0.05$).

The biocompatibility of the scaffolds is closely related to cell attachment, adhesion, and spreading when in contact with them.[29,30] The quality of initial attachment, adhesion, and spreading of cells on the scaffolds will influence the proliferation capacity of cells as well as directional differentiation on them (Figure 4).[30] The CLSM image and quantitative statistics of attached cells indicated that the composite PGH scaffolds surface more conducive to cell adhesion. MC3T3-E1 cells protrude more filopodia and lamellipodia and stretched better on the PGH composite scaffold (Figure 4A, B). The cells integrated better with composite fibers than pure PLGA fibers when cultured for 24 h, which confirmed the results above. Our study indicated that the incorporation of GH biomimetics could significantly improve cytocompatibility of the PLGA scaffold. On account of bone is composed of nanofibrous collagen fibers and HA nanocrystals, the incorporation of GH bone mimetic into PLGA electrospun nanofibers could mimic the component and nanotopography of bone to some extent. Thus, the composite PGH scaffold is more favorable for bone cells adhesion. Various bioactive molecules such as short oligopeptide (RGD) with increased binding specificity to integrins that could enhance cell adhesion,

dx.doi.org/10.1021/am5017792 | ACS Appl. Mater. Interfaces 2014, 6, 9402−9410

spreading, and proliferation.[31] The RGD sequences within gelatin would serve this function. Besides, the hydrophilic characteristic of gelatin is also better for cell adhesion. Bone cells would take very short time to adapt to the composite PGH scaffold microenvironment. The quick bone cell attachment and adhesion on the composite PGH nanofibers gained time for cell survival. Cell spreading starts at the establishment of focal adhesion plaques between the substrate surface and the cell membrane.[32] Therefore, good attachment and adhesion of cell on the scaffolds are the basis for its spreading. The cells stretched better on PGH scaffold confirmed the excellent cytocompatibility. Besides, the single nanofiber may give guidance for cell migration (Figure 4B).

Based on MTT assay, PGH composite scaffold showed improved MC3T3-E1 proliferation compared with the PLGA scaffold (Figure 5). The presence of GH, a bone biomimetics, is more suitable for bone cell growth. The good attachment and adhesion of cells on the PGH scaffolds also contributed to this. However, studies have shown ambiguous descriptions in regards to the effects of hydroxyapatite on the proliferation of osteoblasts. Some earlier reports using HA discs as culture substrate showed an inhibition of proliferation of MC3TE-E1 cells,[33−35] while other reports implied that HA could enhance osteoblasts adhesion and proliferation[36,37] or no influence on cell proliferation.[38] Studies confirmed that calcium phosphate particles, with a diameter smaller than 50 μm, showed cytotoxicity.[39,40] However, nano-HA has been widely used to improve the biocompatibility of electrospun nanofibers to promote adhesion, proliferation, and differentiation of osteoblasts.[11,41−43] These literatures, as well as our study, shared a common feature that a small amount of HA particles were tightly integrated into polymers fibers. This would prevent osteoblasts from ingesting nanohydroxyapatite particles, which may lead to cytotoxicity, and the relatively smooth surface also contributes to cell proliferation. Besides, the RGD peptides within gelatin can regulate the adhesion of osteoblasts to hydroxyapatite then promote cell proliferation.[41,44] Nevertheless, the negative effects of HA on proliferation of bone cells must be concerned. We need to perform an in-depth study to clarify this issue.

The scaffold performed its desired function and generated best cellular or tissue response are the requirements to evaluate its biocompatibility.[1] The osteoinductive activity of scaffolds is crucial for repairing bone defects. Higher expression of osteogenic genes including Runx2, ALP, and Col1 in PGH group (Figure 6) demonstrated that the incorporation of GH biomimetics into PLGA scaffold could efficiently promote the differentiation of BMSCs toward osteoblasts. Early studies demonstrated that milli-molar concentrations of calcium ions could enhance osteogenic differentiation.[45] Thus, calcium ions released from nanohydroxyapatite shall enhance osteogenic differentiation. Furthermore, the significant higher expression of Col1 indicated that the added gelatin have enhanced the biological function of the PLGA polymer during matrix synthesis. Besides, a better initial event can also lead to a series of preferable cell responses, including cell growth, division, and differentiation. The osteoblasts begin to secrete mineral matrix, and mineralization is a marker of maturation. Enhanced calcium binding and matrix deposition were observed in the PGH composite nanofibrous scaffolds due to the GH incorporation (Figure 7). These results confirmed that PGH composite scaffold had better osteo-inductive activity in vitro. Thus, the PGH composite scaffold has potential applications in bone tissue engineering.

The biocompatibility of a scaffold is a prerequisite for medical therapy. It should not elicit any undesirable local or systemic responses in patient.[1] In vivo host responses were assessed after subcutaneous implantation in rat. The degrees of inflammatory reaction observed surrounding the tissues implanted with these scaffolds were distinct. It was found that the degree in inflammatory reaction surrounding the tissue implanted with PGH composites was lighter than pure PLGA scaffold observed at 2-weeks postoperatively (Figure 8). This may due to that the acidic degradation products of PLGA that can induce mass inflammatory cells infiltration and dense fibrous encapsulation, and the buffering effect of HA on the pH decline during the degradation of PLGA which can help to decrease local inflammation. Besides, the generation of acidic degradation products from the same weight of the two scaffolds, PGH composite scaffold was also lower. Thus, this will also serve to decline local inflammation surrounding PGH composite in vivo. Our findings are consistent with previous research partially that the incorporation of HA or calcium phosphate cement into PLGA electrospun fibrous scaffolds had improved biocompatibility.[15] However, this is at the expense of degradation rate of PLGA. When guided damaged tissue repair and regeneration, the degradation rate of engineering scaffolds must match native tissue repair progress to achieve maximum effect. Prematurely degradation of scaffold will lead to poor induction period, while too slow will hinder new tissue ingrowth, thereby impairing tissue healing. Due to rapid degradation rate, the added gelatin may offset the effects on scaffold degradation resulting from HA in vivo.[12] Moreover, the relatively small diameter of the PGH fibers may also benefit for its degradation. However, we need further to investigate the various proportions of PLGA, gelatin and hydroxyapatite to get an appropriate degradation rate in vivo to guide bone regeneration. These results suggested that the composite PGH nanofibers scaffold could be an excellent scaffold for bone tissue engineering.

5. CONCLUSIONS

Our study demonstrated that the incorporation of gelatin/nanohydroxyapatite bone biomimetics into PLGA electrospun nanofibers could facilitates bone cell adhesion, migration, and proliferation, as well as progenitor cells osteogenic differentiation. Moreover, the PGH scaffold also had good performance in vivo. Hence, electrospun PLGA/gelatin/nanohydroxyapatite nanofibrous scaffolds have good biocompatibility and are promising biocomposite scaffolds for bone tissue engineering.

AUTHOR INFORMATION

Corresponding Author

*Tel: 86-431-88796012. Fax: 86-431-88975348. Email: hcsun@mail.jlu.edu.cn.

Author Contributions

‖The manuscript was written through contributions of all authors. All authors have given approval to the final version of the manuscript. D.L. and H.S. contributed equally.

Notes

The authors declare no competing financial interest.

■ ACKNOWLEDGMENTS

The PLGA was offered by Chinese Academy of Sciences Changchun Institute of Applied Chemistry. This study was supported by the National Natural Science Foundation of China (81320108011, 81271111, 30830108), Research Fund for the Doctoral Program of Higher Education of China (233200801830063, 20120061130010), and the Science Technology Program of Jilin Province (201201064).

■ REFERENCES

(1) Williams, D. F. On the Mechanisms of Biocompatibility. *Biomaterials* **2008**, *29*, 2941−2953.
(2) Cai, Y. Z.; Zhang, G. R.; Wang, L. L.; Jiang, Y. Z.; Ouyang, H. W.; Zou, X. H. Novel Biodegradable Three-Dimensional Macroporous Scaffold using Aligned Electrospun Nanofibrous Yarns for Bone Tissue Engineering. *J. Biomed. Mater. Res., Part A* **2012**, *100*, 1187−1194.
(3) Lu, L. X.; Zhang, X. F.; Wang, Y. Y.; Ortiz, L.; Mao, X.; Jiang, Z. L.; Xiao, Z. D.; Huang, N. P. Effects of Hydroxyapatite-Containing Composite Nanofibers on Osteogenesis of Mesenchymal Stem Cells In Vitro and Bone Regeneration In Vivo. *ACS Appl. Mater. Interfaces* **2013**, *5*, 319−330.
(4) Huang, Z. M.; Zhang, Y. Z.; Kotaki, M.; Ramakrishna, S. A Review on Polymer Nanofibers by Electrospinning and Their Applications in Nanocomposites. *Compos. Sci. Technol.* **2003**, *63*, 2223−2253.
(5) Sill, T. J.; von Recum, H. A. Electrospinning: Applications in Drug Delivery and Tissue Engineering. *Biomaterials* **2008**, *29*, 1989−2006.
(6) Shi, J.; Wang, L.; Zhang, F.; Li, H.; Lei, L.; Liu, L.; Chen, Y. Incorporating Protein Gradient into Electrospun Nanofibers as Scaffolds for Tissue Engineering. *ACS Appl. Mater. Interfaces* **2010**, *2*, 1025−1030.
(7) Jang, J. H.; Castano, O.; Kim, H. W. Electrospun Materials as Potential Platforms for Bone Tissue Engineering. *Adv. Drug Delivery Rev.* **2009**, *61*, 1065−1083.
(8) Kai, D.; Jin, G.; Prabhakaran, M. P.; Ramakrishna, S. Electrospun Synthetic and Natural Nanofibers for Regenerative Medicine and Stem Cells. *Biotechnol. J.* **2013**, *8*, 59−72.
(9) Zhang, Y.; Su, B.; Venugopal, J.; Ramakrishna, S.; Lim, C. Biomimetic and Bioactive Nanofibrous Scaffolds from Electrospun Composite Nanofibers. *Int. J. Nanomed.* **2007**, *2*, 623−638.
(10) Gunatillake, P. A.; Adhikari, R. Biodegradable Synthetic Polymers for Tissue Engineering. *Eur. Cells Mater.* **2003**, *5*, 1−16.
(11) Ngiam, M.; Liao, S.; Patil, A. J.; Cheng, Z.; Chan, C. K.; Ramakrishna, S. The Fabrication of Nano-hydroxyapatite on PLGA and PLGA/Collagen Nanofibrous Composite Scaffolds and Their Effects in Osteoblastic Behavior for Bone Tissue Engineering. *Bone* **2009**, *45*, 4−16.
(12) Lee, J. B.; Kim, S. E.; Heo, D. N.; Kwon, I. K.; Choi, B. J. In Vitro Characterization of Nanofibrous PLGA/Gelatin/Hydroxyapatite Composite for Bone Tissue Engineering. *Macromol. Res.* **2010**, *18*, 1195−1202.
(13) Jose, M. V.; Thomas, V.; Johnson, K. T.; Dean, D. R.; Nyairo, E. Aligned PLGA/HA Nanofibrous Nanocomposite Scaffolds for Bone Tissue Engineering. *Acta Biomater.* **2009**, *5*, 305−315.
(14) Jiang, L. M.; Sun, H. Z.; Yuan, A. L.; Zhang, K.; Li, D. W.; Li, C.; Shi, C.; Li, X. W.; Gao, K.; Zheng, C. Y.; Yang, B.; Sun, H. C. Enhancement of Osteoinduction by Continual Simvastatin Release from Poly(lactic-co-glycolic acid)-Hydroxyapatite-Simvastatin Nanofibrous Scaffold. *J. Biomed. Nanotechnol.* **2013**, *9*, 1921−1928.
(15) Ji, W.; Yang, F.; Seyednejad, H.; Chen, Z.; Hennink, W. E.; Anderson, J. M.; van den Beuckena, J. J. J. P.; Jansen, J. A. Biocompatibility and Degradation Characteristics of PLGA-Based Electrospun Nanofibrous Scaffolds with Nanoapatite Incorporation. *Biomaterials* **2012**, *33*, 6604−6614.
(16) Liu, W. Y.; Lipner, J.; Xie, J.; Manning, C. N.; Thomopoulos, S.; Xia, Y. Nanofiber Scaffolds with Gradients in Mineral Content for Spatial Control of Osteogenesis. *ACS Appl. Mater. Interfaces* **2014**, *6*, 2842−2849.
(17) Lee, J. H.; Rim, N. G.; Jung, H. S.; Shin, H. Control of Osteogenic Differentiation and Mineralization of Human Mesenchymal Stem Cells on Composite Nanofibers Containing Poly[lactic-co-(glycolic acid)] and Hydroxyapatite. *Macromol. Biosci.* **2010**, *10*, 173−182.
(18) Kim, H. W.; Song, J. H.; Kim, H. E. Nanofiber Generation of Gelatin−Hydroxyapatite Biomimetics for Guided Tissue Regeneration. *Adv. Funct. Mater.* **2005**, *15*, 1988−1994.
(19) Hulmes, D.; Wess, T. J.; Prockop, D. J.; Fratzl, P. Radial Packing, Order, and Disorder in Collagen Fibrils. *Biophys. J.* **1995**, *68*, 1661−1670.
(20) Chang, M. C.; Ko, C. C.; Douglas, W. H. Preparation of Hydroxyapatite−Gelatin Nanocomposite. *Biomaterials* **2003**, *24*, 2853−2862.
(21) Jansen, J.; Dhert, W.; Van der Waerden, J.; Von Recum, A. Semi-quantitative and Qualitative Histologic Analysis Method for the Evaluation of Implant Biocompatibility. *J. Invest. Surg.* **1994**, *7*, 123−134.
(22) Link, D. P.; van den Dolder, J.; van den Beucken, J. J.; Cuijpers, V. M.; Wolke, J. G.; Mikos, A. G.; Jansen, J. A. Evaluation of the Biocompatibility of Calcium Phosphate Cement/PLGA Microparticle Composites. *J. Biomed. Mater. Res., Part A* **2008**, *87*, 760−769.
(23) Griffith, L. G.; Naughton, G. Tissue Engineering—Current Challenges and Expanding Opportunities. *Science* **2002**, *295*, 1009−1014.
(24) Ki, C. S.; Baek, D. H.; Gang, K. D.; Lee, K. H.; Um, I. C.; Park, Y. H. Characterization of Gelatin Nanofiber Prepared from Gelatin−Formic Acid Solution. *Polymer* **2005**, *46*, 5094−5102.
(25) El-Ghannam, A. R.; Ducheyne, P.; Risbud, M.; Adams, C. S.; Shapiro, I. M.; Castner, D.; Golledge, S.; Composto, R. J. Model Surfaces Engineered with Nanoscale Roughness and RGD Tripeptides Promote Osteoblast Activity. *J. Biomed. Mater. Res., Part A* **2004**, *68*, 615−627.
(26) Von Hippel, P. H. The Macromolecular Chemistry of Gelatin. *J. Am. Chem. Soc.* **1965**, *87*, 1824−1824.
(27) Kim, H. W.; Lee, H. H.; Knowles, J. C. Electrospinning Biomedical Nanocomposite Fibers of Hydroxyapatite/Poly (lactic acid) for Bone Regeneration. *J. Biomed. Mater. Res., Part A* **2006**, *79*, 643−649.
(28) Altankov, G.; Groth, T. Reorganization of Substratum-Bound Fibronectin on Hydrophilic and Hydrophobic Materials is Related to Biocompatibility. *J. Mater. Sci.: Mater. Med.* **1994**, *5*, 732−737.
(29) Ratner, B. D.; Horbett, T.; Hoffman, A. S.; Hauschka, S. D. Cell Adhesion to Polymeric Materials: Implications with Respect to Biocompatibility. *J. Biomed. Mater. Res., Part A* **1975**, *9*, 407−422.
(30) Anselme, K. Osteoblast Adhesion on Biomaterials. *Biomaterials* **2000**, *21*, 667−681.
(31) Kantlehner, M.; Schaffner, P.; Finsinger, D.; Meyer, J.; Jonczyk, A.; Diefenbach, B.; Nies, B.; Hölzemann, G.; Goodman, S. L.; Kessler, H. Surface Coating with Cyclic RGD Peptides Stimulates Osteoblast Adhesion and Proliferation as well as Bone Formation. *ChemBiochem* **2000**, *1*, 107−114.
(32) Cavalcanti-Adam, E. A.; Volberg, T.; Micoulet, A.; Kessler, H.; Geiger, B.; Spatz, J. P. Cell Spreading and Focal Adhesion Dynamics are Regulated by Spacing of Integrin Ligands. *Biophys. J.* **2007**, *92*, 2964−2974.
(33) Deligianni, D. D.; Katsala, N. D.; Koutsoukos, P. G.; Missirlis, Y. F. Effect of Surface Roughness of Hydroxyapatite on Human Bone Marrow Cell Adhesion, Proliferation, Differentiation and Detachment Strength. *Biomaterials* **2000**, *22*, 87−96.
(34) Shu, R.; McMullen, R.; Baumann, M.; McCabe, L. Hydroxyapatite Accelerates Differentiation and Suppresses Growth of MC3T3-E1 Osteoblasts. *J. Biomed. Mater. Res., Part A* **2003**, *67*, 1196−1204.
(35) Oreffo, R. O.; Driessens, F.; Planell, J. A.; Triffitt, J. T. Growth and Differentiation of Human Bone Marrow Osteoprogenitors on

Novel Calcium Phosphate Cements. *Biomaterials* **1998**, *19*, 1845−1854.
(36) Okamoto, K.; Matsuura, T.; Hosokawa, R.; Akagawa, Y. RGD Peptides Regulate the Specific Adhesion Scheme of Osteoblasts to Hydroxyapatite but not to Titanium. *J. Dent. Res.* **1998**, *77*, 481−487.
(37) Maxian, S. H.; Di Stefano, T.; Melican, M. C.; Tiku, M. L.; Zawadsky, J. P. Bone Cell Behavior on Matrigel-Coated Ca/P Coatings of Varying Crystallinities. *J. Biomed. Mater. Res., Part A* **1998**, *40*, 171−179.
(38) Ozawa, S.; Kasugai, S. Evaluation of Implant Materials (Hydroxyapatite, Glass-Ceramics, Titanium) in Rat Bone Marrow Stromal Cell Culture. *Biomaterials* **1996**, *17*, 23−29.
(39) Higashi, T.; Okamoto, H. Influence of Particle Size of Hydroxyapatite as a Capping Agent on Cell Proliferation of Cultured Fibroblasts. *J. Endodont.* **1996**, *22*, 236−239.
(40) Sun, J. S.; Tsuang, Y. H.; Chang, WH. S.; Li, J.; Liu, H. C.; Lin, F. H. Effect of Hydroxyapatite Particle Size on Myoblasts and Fibroblasts. *Biomaterials* **1997**, *18*, 683−690.
(41) Song, J. H.; Kim, H. E.; Kim, H. W. Electrospun Fibrous Web of Collagen−Apatite Precipitated Nanocomposite for Bone Regeneration. *J. Mater. Sci.: Mater. Med.* **2008**, *19*, 2925−2932.
(42) Prabhakaran, M. P.; Venugopal, J.; Ramakrishna, S. Electrospun Nanostructured Scaffolds for Bone Tissue Engineering. *Acta biomater.* **2009**, *5*, 2884−2893.
(43) Ravichandran, R.; Venugopal, J. R.; Sundarrajan, S.; Mukherjee, S.; Ramakrishna, S. Precipitation of Nanohydroxyapatite on PLLA/PBLG/Collagen Nanofibrous Structures for the Differentiation of Adipose Derived Stem Cells to Osteogenic Lineage. *Biomaterials* **2012**, *33*, 846−855.
(44) Hennessy, K. M.; Clem, W. C.; Phipps, M. C.; Sawyer, A. A.; Shaikh, F. M.; Bellis, S. L. The Effect of RGD Peptides on Osseointegration of Hydroxyapatite Biomaterials. *Biomaterials* **2008**, *29*, 3075−3083.
(45) Sugimoto, T.; Kanatani, M.; Kano, J.; Kaji, H.; Tsukamoto, T.; Yamaguchi, T.; Fukase, M.; Chihara, K. Effects of High Calcium Concentration on the Functions and Interactions of Osteoblastic Cells and Monocytes and on the Formation of Osteoclast-like Cells. *J. Bone Miner. Res.* **1993**, *8*, 1445−1452.